

Hysteretic internal fields and critical currents in polycrystalline superconductors

M. N. Kunchur^{a)}

Department of Physics and Astronomy, University of South Carolina, Columbia, South Carolina 29208

T. R. Askew

Department of Physics, Kalamazoo College, Kalamazoo, Michigan 49006 and Materials Science Division, Argonne National Laboratory, Illinois 60439

(Received 6 July 1998; accepted for publication 16 September 1998)

The transport critical current J_c in a polycrystalline superconductor is a hysteretic function of applied magnetic field H_0 due to flux trapping by grains. This effect has been observed by several groups and attempts have been made to calculate the intergranular field H_i as a function of the applied H_0 in terms of an effective geometrical demagnetization factor D . In general a first-principles calculation of D is very difficult, and furthermore, D is not constant but is itself a hysteretic function of H_0 . We develop a self-consistent scheme to extract the D and H_i directly from the $J_c(H_0)$ data itself. Our model exploits the fact that there are two field ranges for which the demagnetizing field is a simple function of H_0 . At low virgin fields, in the Meissner state, the susceptibility $\chi_v \approx -1/4\pi$ is well defined, leading to a multiplicative correction: $H_i = H_0 / (1 + D4\pi\chi_v)$. For fields that have returned from high values, a complete critical state is established and M is well defined—although χ_v is unknown. This leads to an additive correction: $H_i = H_0 - D4\pi M$ for the total field. By matching J_c data in increasing and decreasing fields that satisfy these special cases, it is possible to extract the relevant parameters of the problem without detailed knowledge of the demagnetization geometry. We use this model to analyze data measured on sintered $\text{YBa}_2\text{Cu}_3\text{O}_7$ superconductive rods. © 1998 American Institute of Physics. [S0021-8979(98)03824-9]

I. INTRODUCTION

The phenomena that govern the critical current density J_c , and its dependence on field are important aspects in the field of high- T_c superconductors, both from a fundamental standpoint as well as for applications. The field sensitivity of J_c is especially pronounced in bulk ceramic materials¹ where it often shows a precipitous drop followed by a somewhat gentler decrease at high fields. In addition it has been found in many investigations¹⁻¹⁷ that J_c is a bivalued function of the applied field H_0 .

Figure 1 shows our data on $\text{YBa}_2\text{Cu}_3\text{O}_7$ ceramic rods illustrating the effect. The virgin curve (circles) represents the field dependence of J_c when the sample is cooled in zero field to the desired temperature and the field is then increased isothermally (H_0^\uparrow). The field is taken to some turning value H_t after which it is decreased back to zero. The squares show data in decreasing field (H_0^\downarrow) for a turning field of 200 Oe. Because of flux trapped within the grains the internal field H_i at the grain boundaries is different for a given applied field H_0 , for the two field-change directions. The data shown by the crosses are for $H_t = 1000$ Oe. Because the amount of trapped flux increases monotonically with H_t , so does the enhancement in J_c . The magnitude of the enhancement finally saturates at some value of the turning field $H_t = H_{ts}$, when the grain is in a complete critical state. In the remainder of the discussion, whenever we talk about increasing

field curves and data, it will always be assumed that the field was increased from the virgin (zero-field-cooled) condition.

One of the models^{2,3} proposed to explain the hysteretic J_c invokes irreversible flux trapping within the grains accompanied by hysteresis in demagnetizing fields at the grain boundaries. Some qualitative features have been satisfactorily explained in this way by the previous authors. Mune *et al.*¹⁸ and Navarro and Campbell¹⁹ have used the mean-value theorem and effective medium approaches to treat the problem. One challenge in calculating the internal field is that, in general, a first-principles calculation of the effective demagnetization factor D , and the resultant demagnetizing field is very difficult. Furthermore, D is not constant but is itself a hysteretic function of H_0 , because of the changing flux distributions within the grains.

In this article we explore the ideas of flux trapping and compression further and develop a self-consistent scheme for extracting D and H_i . The scheme exploits a mathematical simplification in the demagnetization-correction equations that occurs for certain field conditions. This allows us to derive expressions for the true intrinsic field dependence of the critical current $J_c(H_i)$ from the increasing-field $J_c(H_0^\uparrow)$ and decreasing-field $J_c(H_0^\downarrow)$ curves. Knowledge of the intrinsic function $J_c(H_i)$ is needed for understanding the underlying physical mechanisms which cause the field dependence of J_c across grain boundaries and weak links. As demonstrated in previous work,^{2,3} it will be assumed that the self field of the measuring current is negligible and that most of

^{a)}Electronic mail: kunchur@cosm.sc.edu

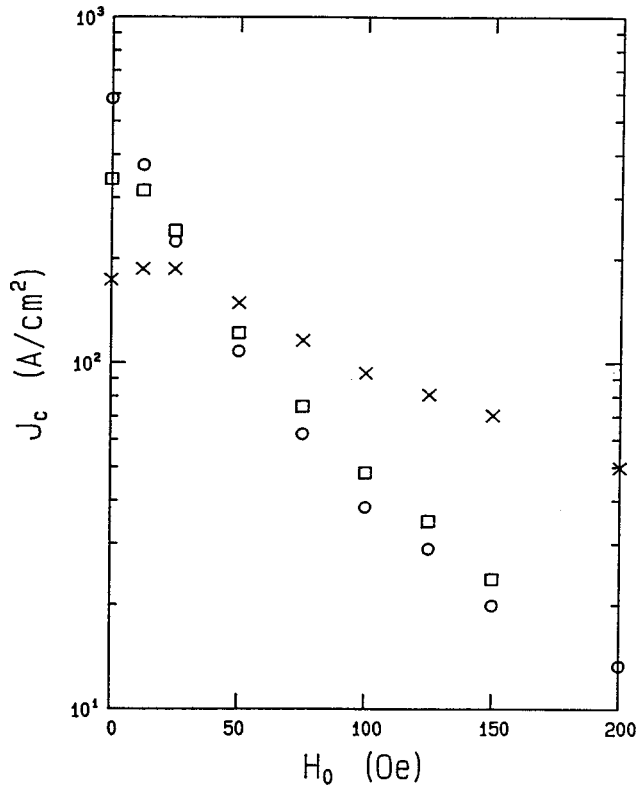


FIG. 1. Hysteretic field dependence of the critical current density J_c in a $\text{YBa}_2\text{Cu}_3\text{O}_7$ ceramic rod (sample A) at 83.4 K. The circles show J_c in an increasing applied field H_0 , for a virgin (zero-field-cooled) sample. The squares show J_c as a function of the field as it is decreased after being taken up to a turning field H_t of 200 Oe. The crosses show decreasing-field data for $H_t=1000$ Oe. For a given value of H_0 , J_c has a value that depends on the direction of field change as well as the value of the turning field. The enhancement of J_c with increasing H_t saturates above $H_t=H_{ts}$, which is 900 Oe at this temperature.

the flux trapping occurs within the grains and not by bulk screening currents. Also demagnetization effects due to the overall sample shape are not considered here. (The measurements we analyze here were done on thin rods in parallel field for which the overall demagnetization is negligible anyway.)

II. EXPERIMENTAL DETAILS

The samples were sintered rods of $\text{YBa}_2\text{Cu}_3\text{O}_7$ made by the oxide-precursors route. They are characterized by a uniform fine grain structure and connected porosity, and are relatively immune to microcracking. Their length is typically 30 times the diameter (0.7–0.9 mm), facilitating accurate four-probe measurements.

The critical currents were measured by a pulsed four-probe method. The current pulses were 2 ms in duration with a duty cycle of less than a percent. The contacts were 1 cm apart and a 2 μV criterion was used to define J_c . Further information on the sample preparation and characterization, and on the measurement technique can be found in Refs. 7 and 20, and references therein.

III. THEORETICAL MODEL

There are several ranges of the applied field over which it is possible to derive simple expressions for the internal field H_i in terms of the applied H_0 and demagnetization, in a way that provides useful information without requiring detailed knowledge of actual demagnetizing factors or current-flow morphology. This approach seeks to derive the dependencies $H_i(H_0^\uparrow)$ and $H_i(H_0^\downarrow)$, of the internal field on the increasing (H_0^\uparrow) and decreasing (H_0^\downarrow) applied fields, and thereby understand the behavior of $J_c(H_0)$ in a somewhat quantitative manner without addressing the physical reasons for the field dependence at the grain boundaries. The latter has been attributed both to Josephson-junction weak links²¹ as well as to regions of easy flux flow²² at the grain boundaries. Note that the actual local fields H_l at various grain boundaries will all vary differently from each other. This may cause the configuration of current pathways to change with field. A simplifying assumption made in this model is that all the individual changes taking place on the microscopic level need not be considered separately and that the net behavior can be described in terms of the average macroscopic quantities J_c and H_i .

There are two situations for which the demagnetizing field is a simple function of H_0 . One is when the material has a known field-independent susceptibility ($\chi_v = \text{const.}$), the other is when the magnetization M is well defined. The respective relations for those two cases are

$$H_i = H_0 / (1 + D4\pi\chi_v) \quad (1)$$

and

$$H_i = H_0 - D4\pi M. \quad (2)$$

The first occurs in the Meissner state when M is unknown (because H_i is not known) but χ_v is well defined ($-1/4\pi$). The second occurs for fields at which the grains are completely penetrated by flux and then the susceptibility is undefined but M can be calculated from the Bean²³ or other²⁴ critical state models. These models give expressions for the flux density as a function of the depth from the surface $B(x)$; the average magnetization is then obtained from the local quantity ($4\pi M = B - H$) by integration over the volume. In the present work, we will take²⁵ $B(x) = H_0 - H_{c1} - 4\pi J_c x/c$, in which linear profiles are assumed (because of the smallness of the grains this is a reasonable approximation) and the lower-critical-field term (H_{c1}) accounts for the reversible component of M . Note that D will differ for each field case since the flux distribution is not the same. We now obtain the explicit expressions for various field cases.

(1) For a sample cooled in zero field (ZFC), as the field is initially increased from zero the grains are in the Meissner state and exclude flux completely causing excess flux to be compressed into the intergranular spaces.^{2,26,27} The flux-density distribution within the grain is uniformly zero everywhere as shown in Fig. 2(a). Even for H_i slightly above H_{c1} —although flux penetration has begun—most of the grain is still flux free so that the average susceptibility remains $\chi_v \approx -1/4\pi$. From Eq. (1), we get

$$H_i = H_0^\uparrow / (1 - D_1). \quad (3)$$

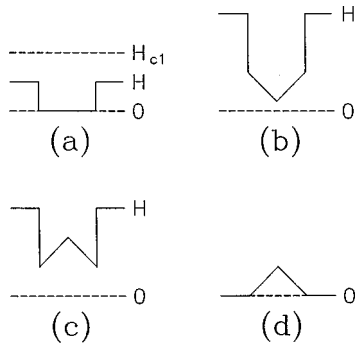


FIG. 2. Flux-density distributions inside a superconducting grain in an external field H . In (a) a virgin increasing field less than H_{c1} is applied. In (b) a virgin field $H > H^*$ is applied so that the grain is completely penetrated by flux. In (c) the field is cycled to a high value $H > H_{ts}$ and reduced so as to trap flux. In (d) the field is now reduced to zero.

Thus the applied field is simply scaled by the factor $= 1/(1 - D_1)$. Because the degree of flux exclusion is largest at low fields, one expects the demagnetization to be the largest for this field range.

(2) Further on the increasing curve, flux begins to penetrate the grains when $H_i > H_{c1}$ and they become fully penetrated when $H_i = H^* = H_{c1} + 4\pi J_{ci}R/3c$. For $H_i \geq H^*$, the magnetization remains roughly constant at $4\pi M = -H_{c1} - 4\pi J_{ci}R/3c$ (R is an average effective grain radius and J_{ci} is the intragranular critical current density). The flux-density profile for this field regime is shown in Fig. 2(b). Note that the magnetization can be regarded as the sum of two components: one is a uniform plateau of magnetization $-H_{c1}$, the other is a cone shaped profile for which the average magnetization is $-4\pi J_{ci}R/3c$. For the first homogeneous component, the demagnetization factor will be the previous D_1 ; for the inhomogeneous part, the demagnetization factor will have a different value D_2 . Because the second conical component is concentrated towards the center of the grain the effective radius of that core is smaller. This in effect increases the intergrain separation, lowering the extent of flux compression. D_2 will therefore be smaller than D_1 . In this field range M , and not χ_v , is well defined and H_i can thus be obtained from Eq. (2) in terms of D_1 and D_2 :

$$H_i = H_0^\uparrow + D_1 H_{c1} + D_2 4\pi J_{ci}R/3c. \quad (4)$$

The enhancement of H_i over H_0 is smaller here than in the previous field range [Eq. (3)].

(3) When H_i is increased up to a certain value (the turning field H_t) above H_{c1} and decreased, a remanent moment is trapped. The moment becomes increasingly positive as the turning field is increased, the effect finally saturating at $H_t = H_{ts}$ with H_{ts} given by²⁸

$$H_{ts} = H_{c1} + 8\pi J_{ci}R/3c. \quad (5)$$

H_{ts} is a monotonically decreasing function of temperature through its dependence on H_{c1} and J_{ci} . In fact from the known temperature dependencies of $H_{c1}(T)$ and $J_{ci}(T)$ (after suitable orientation averaging), it is possible to calculate that dependence and quantitatively compare it with the measured values of H_{ts} at different temperatures.

Within the field range $H_{c1} \leq H_i \leq H_t - 8\pi J_{ci}R/3c$, for $H_t > H_{ts}$, the magnetization is given by $4\pi M = -H_{c1} + 4\pi J_{ci}R/3c$ and the associated flux-density distribution is shown in Fig. 2(c). As for the previous field range, the magnetization can be conveniently split into two components: the uniform plateau of value, H_{c1} (demagnetization D_1) and the inverted cone of average value $4\pi J_{ci}R/3c$ (demagnetization D_2). Whence from Eq. (2) the internal field is

$$H_i = H_0^\downarrow + D_1 H_{c1} - D_2 4\pi J_{ci}R/3c. \quad (6)$$

(4) Finally, when the field is decreased well below H_{c1} —after having increased above H_{ts} —only the remanent magnetization [Fig. 2(d)] remains given by the well-known formula $M = J_{ci}R/3c$ and the internal field is

$$H_i = H_0^\downarrow - D_2 4\pi J_{ci}R/3c. \quad (7)$$

As explained earlier, one expects the demagnetization to drop after crossing from field-range 1 [Eq. (3)] to field-range 2 [Eq. (4)]. Because of this H_i will vary rapidly with H_0 at lower fields steepening the initial $J_c(H_0)$ slope; after crossing over into field-range 2, H_i and therefore J_c will vary more slowly with H_0 . This may be partially responsible for the exaggerated initial drop in J_c at low fields followed by the more gradual decrease at higher fields observed by various authors.²⁹ The behavior is usually attributed to a destruction of weak links at low fields, and a crossover to parallel, more robust, conduction channels at higher fields. However, part of the change in behavior may be merely due to a change in the demagnetization rather than to a change in the dominant conduction channels. For decreasing fields, the demagnetization does not undergo any abrupt changes and $J_c(H_0)$ ought to be a smooth function of the applied field. This distinction in the increasing- and decreasing-field cases is indeed borne out by the data in Fig. 1 represented by circles and crosses, respectively. (Also see, for example, Fig. 1(a) of Ref. 26.)

IV. ANALYSIS

The model presented above will now be used to analyze the $J_c(H_0)$ data in the following way: Take values of H_0^\uparrow corresponding to certain J_c 's on the increasing-field curve and plot them against the corresponding values of H_0^\downarrow on the decreasing-field curve (considering only turning fields that have exceeded the saturation values) which have the same J_c 's. The two sets of values should satisfy Eqs. (3) and (6) respectively, and presumably each point on the plot corresponds to a pair of values $(H_0^\uparrow, H_0^\downarrow)$ which produce the same H_i , since $J_c(H_0^\uparrow) = J_c(H_0^\downarrow)$ and we have assumed that J_c is a single-valued function of H_i . From Eqs. (3) and (6) we expect a linear relation between H_0^\uparrow and H_0^\downarrow :

$$H_0^\uparrow = H_0^\downarrow / (1 - D_1) + (-D_1 H_{c1} + D_2 4\pi J_{ci}R/3c). \quad (8)$$

The slope and the intercept together give D_1 and D_2 , the effective demagnetization factors for the H_0^\uparrow and H_0^\downarrow cases. The intercept's sign can be either positive or negative depending on the relative magnitudes of $D_1 H_{c1}$ and $D_2 4\pi J_{ci}R/3c$. D_1 will depend somewhat on the sample's morphology: a more porous sample will have lower com-

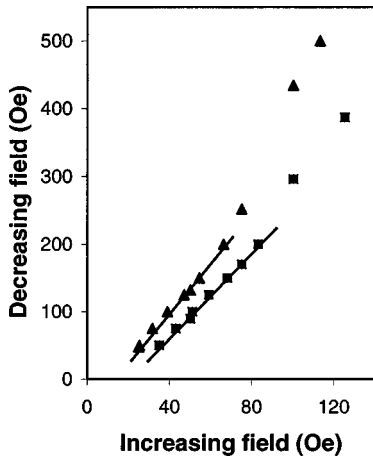


FIG. 3. Decreasing applied field (H_0^\downarrow) values plotted against the corresponding increasing applied field (H_0^\uparrow) values that have the same J_c . Squares and triangles represent data for samples A and B, respectively. Straight lines are linear fits to the low field data. $T=77.3$ K, $H_i=5000$ Oe, and $H_{1s}=3000$ Oe for both sets.

pression. In a given sample, temperature dependence of D_1 will indicate how stable the configuration of dominant current pathways is. Note that although Eq. (8) can, in principle, yield both D_1 and D_2 , only the extracted value of D_1 is reliable since it relates directly to the slope of Eq. (8) without any additional parameters. D_2 , on the other hand, depends not only on the intercept, but on four additional parameters (D_1 , H_{c1} , J_{ci} , and R). Fortunately, D_2 's explicit value does not enter the calculation of the final quantities of interest that this model tries to extract (e.g., J_{ci} and H_i); for that only the entire intercept of Eq. (8) matters. Hence in the remainder of the analysis we will not bother with D_2 explicitly.

Figure 3 shows such a plot for data measured on two samples at $T=77.3$ K. Notice the linear relationship between H_0^\uparrow and H_0^\downarrow at low fields, predicted by Eq. (8). From the slopes we find that $D_1=0.68$ for sample A and $D_1=0.71$ for sample B, both roughly independent (within 5%) of temperature (measured at 77.3, 83.4, and 87.4 K). The intercepts are -60 and -35 Oe for the two samples, respectively, again not changing much (within 10%) with T . Thus we see that the current-flow morphology is relatively stable. At the highest fields, the plots in Fig. 3 show a deviation from linearity. This is due to a crossover to field-insensitive current carrying channels as discussed earlier.

From the measured slope $1/(1-D_1)$, and intercept $(-D_1H_{c1}+D_24\pi J_{ci}R/3c)$, one can now use Eqs. (3) or (6) to obtain the average internal field H_i , and hence the intrinsic field dependence $J_c(H_i)$. Figure 4 shows such plots of J_c versus the corrected internal field H_i , as well as J_c versus the raw H_0^\uparrow and H_0^\downarrow values. One important conclusion that arises from this analysis is that $J_c(H_0^\downarrow)$ is closer to the intrinsic $J_c(H_i)$ than $J_c(H_0^\uparrow)$, because of the much smaller demagnetizing field in field range 3 governing H_0^\downarrow . However, because of the additive way in which Eq. (6) converts H_0^\downarrow to H_i , $J_c(H_0^\downarrow)$ has an erroneous exponent. H_0^\uparrow , on the other hand, is corrected multiplicatively in Eq. (3) and consequently $J_c(H_0^\uparrow)$ has the same power-law exponent as the in-

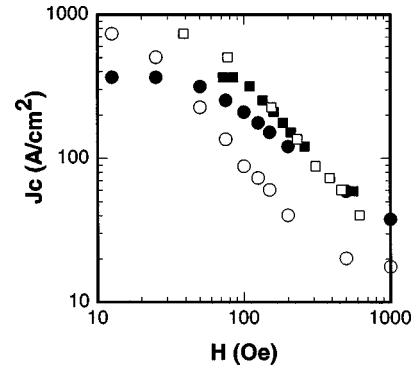


FIG. 4. Squares show critical current density J_c vs the corrected internal field for sample A. Circles show J_c plotted against the raw values of applied field. Increasing and decreasing field data are denoted by open and closed symbols, respectively. $T=77.3$ K, $H_i=5000$ Oe, and $H_{1s}=3000$ Oe. Note that $J_c(H_0^\downarrow)$ has the same slope as the intrinsic curve but is shifted to a larger extent compared with $J_c(H_0^\uparrow)$. This is a consequence of the larger demagnetization for this field range combined with the multiplicative mathematical form of the correction.

trinsic $J_c(H_i)$. This is evident in Fig. 4 where $J_c(H_0^\downarrow)$ has the same slope as $J_c(H_i)$.

Finally, Eq. (5) estimates the saturation turning field H_{1s} , in terms of the intrinsic parameters H_{c1} and J_{ci} (intragranular J_c). For both samples A and B, the measured H_{1s} 's at the three temperatures (77.3, 83.4, and 87.4 K) were about 3000, 900, and 500 Oe, respectively, and the mean grain size was $R\approx 2.5$ μm . Using $H_{c1}=600(1-T/T_c)$ (from Ref. 30) Eq. (5) yields $J_{ci}(T=77.3\text{ K})=4.5\times 10^6$ A/cm², $J_{ci}(T=83.4\text{ K})=1.3\times 10^6$ A/cm², and $J_{ci}(T=87.4\text{ K})=0.7\times 10^6$ A/cm², which are in the range of expected intragranular values for J_c in $\text{YBa}_2\text{Cu}_3\text{O}_7$ at these temperatures.

V. CONCLUSION

In summary, a scheme is presented for analyzing hysteretic $J_c(H_0)$ data in a self-consistent way that allows the extraction of three useful pieces of information: the effective average demagnetization factor, the intrinsic dependence of the overall J_c on the average intergranular field, and the intragranular J_{ci} . These quantities in turn reflect the porosity and connectivity of the sample, the type of interface between grains, the dominant physical mechanisms governing intergranular conduction, and the quality of the grains themselves. Although we consider here only the hysteresis in J_c , it is clear that the same model can be applied with some modification to other hysteretic properties such as V - H characteristics² and microwave measurements.³¹ Conduction in granular superconductors is of revived recent interest because practical high temperature superconductor conductors being presently developed (e.g., BSCCO/Ag tapes or deposited conductors on polycrystalline substrates) do not consist of single crystalline domains.

ACKNOWLEDGMENTS

The authors would like to thank R. B. Flippen and D. K. Christen for useful discussions and proofreading of the manuscript. This work was supported in part by E. I.

du Pont de Nemours and Company, Inc. and the U.S. Department of Energy Office of Advanced Utility Concepts—Superconductivity Program.

- ¹D. W. Murphy, D. W. Johnson, Jr., S. Jin, and R. E. Howard, *Science* **241**, 922 (1988).
- ²J. E. Evetts and B. A. Glowacki, *Cryogenics* **28**, 641 (1988).
- ³K. Kwasnitza and Ch. Widmer, *Cryogenics* **29**, 1035 (1989).
- ⁴K. Matsuzaki, A. Inue, H. Kimura, K. Aoki, and T. Masumoto, *Jpn. J. Appl. Phys., Part 1* **26**, 1310 (1987); M. Okada, A. Okayama, T. Marimoto, T. Matsumoto, K. Aihara, and S. Matsuda, *ibid.* **27**, 185 (1988); J. Chadwick, G. R. Court, and D. H. Jones, *Solid State Commun.* **1**, 19 (1989); K. Watanabe, K. Noto, H. Morita, H. Fujimori, K. Mizuno, T. Aomine, B. Ni, T. Matsushita, K. Yamafuji, and Y. Muto, *Cryogenics* **29**, 263 (1989).
- ⁵T. R. Askew and R. B. Flippen, *Mater. Res. Soc. Symp. Proc.* **169**, 939 (1990).
- ⁶P. K. Mishra, G. Ravikumar, P. Chaddah, S. Kumar, and B. A. Dasannacharya, *Jpn. J. Appl. Phys., Part 2* **29**, L1612 (1990).
- ⁷T. R. Askew, R. B. Flippen, K. J. Leary, and M. N. Kunchur, *J. Mater. Res.* **6**, 1135 (1991).
- ⁸D. Abukay, H. Nakano, and L. Rinderer, *Solid State Commun.* **79**, 573 (1991).
- ⁹K. Vad, S. Meszaros, N. Hegman, and G. Halasz, *J. Supercond.* **5**, 491 (1992).
- ¹⁰W. F. Huang, K. J. Hung, and J. G. Shen, *Physica C* **208**, 7 (1993).
- ¹¹K.-H. Muller and D. N. Matthews, *IEEE Trans. Appl. Supercond.* **3**, 1229 (1993).
- ¹²S. Q. Guo, Y. C. Lan, B. Ye, R. Zeng, Y. R. Zhou, M. Zhou, and L. Xiao, *Physica C* **235**, 3025 (1994).
- ¹³A. Marx, K.-D. Huseman, B. Mayer, T. Nissel, R. Gross, M. A. J. Verhoeven, and G. J. Gerritsma, *Appl. Phys. Lett.* **64**, 241 (1994).
- ¹⁴N. S. Belousov, L. L. Makarshi, and V. N. Parmon, *Physica C* **235**, 3009 (1994).
- ¹⁵W. D. Lee, L. Horng, T. J. Yang, and Chiou Bi-Shiou, *J. Appl. Phys.* **77**, 3942 (1995).
- ¹⁶E. Altshuler, P. Mune, J. Musa, J. L. Gonzalez, O. Ares, and C. Hart, *J. Supercond.* **8**, 781 (1995).
- ¹⁷C. Sarma, G. Shindler, D. G. Haase, C. C. Koch, and A. I. Kingon, *Cryogenics* **36**, 123 (1996).
- ¹⁸P. Mune, E. Altshuler, and J. Musa, *Physica C* **246**, 55 (1995).
- ¹⁹R. Navarro and L. J. Campbell, *Supercond. Sci. Technol.* **5**, S121 (1992).
- ²⁰M. N. Kunchur, *Mod. Phys. Lett. B* **9**, 399 (1995).
- ²¹R. L. Peterson and J. W. Ekin, *Phys. Rev. B* **37**, 9848 (1988).
- ²²D. P. Hampshire, J. A. S. Ikeda, and Y. M. Chiang, *Phys. Rev. B* **40**, 8818 (1989).
- ²³C. P. Bean, *Phys. Rev. Lett.* **8**, 250 (1962).
- ²⁴Y. B. Kim, C. F. Hempstead, and A. R. Strnad, *Phys. Rev. Lett.* **9**, 306 (1962); *Phys. Rev.* **129**, 528 (1963); W. A. Fietz, M. R. Beasley, J. Silcox, and W. W. Webb, *ibid.* **136**, A335 (1964); A. M. Campbell and J. E. Evetts, *Adv. Phys.* **21**, 199 (1972).
- ²⁵For figures of typical internal flux-density profiles and external flux distributions see Fig. 10 of Ref. 2; also see P. G. de Gennes, *Superconductivity of Metals and Alloys* (Benjamin, New York, 1966); and H. Ullmaier, *Irreversible Properties of Type II Superconductors*, Springer Tracts in Modern Physics (Springer, Berlin, 1975).
- ²⁶U. Dai, G. Deutscher, C. Lacour, F. Laher-Lacour, P. Mocaer, and M. Lagues, *Appl. Phys. Lett.* **56**, 1284 (1990).
- ²⁷G. Waysand, *Europhys. Lett.* **5**, 73 (1988).
- ²⁸For a discussion of these concepts along with illuminating figures, see M. Tinkham, *Introduction to Superconductivity* (McGraw-Hill, New York, 1975).
- ²⁹J. W. Ekin, H. R. Hart, Jr., and A. R. Gaddipati, *J. Appl. Phys.* **68**, 2285 (1990), and references therein.
- ³⁰L. Krusin-Elbaum, A. P. Malozemoff, Y. Yeshurun, D. C. Cronemeyer, and F. Holtzberg, *Phys. Rev. B* **39**, 2936 (1989).
- ³¹E. J. Pakulis and T. Usada, *Phys. Rev. B* **37**, 5940 (1988).